

Four-coloured Spin-wave Excitations in Multiferroic Materials

I. Kézsmárki,^{1,2} D. Szaller,¹ S. Bordács,³ H. Murakawa,⁴ Y. Tokura,^{3,4} H. Engelkamp,⁵ T. Rõõm,⁶ and U. Nagel⁶

¹*Department of Physics, Budapest University of Technology and Economics, 1111 Budapest, Hungary*

²*Condensed Matter Research Group of the Hungarian Academy of Sciences, 1111 Budapest, Hungary*

³*Quantum-Phase Electronics Center and Department of Applied Physics, University of Tokyo, Tokyo 113-8656, Japan*

⁴*RIKEN Center for Emergent Matter Science (CEMS), Wako 351-0198, Japan*

⁵*High Field Magnet Laboratory, Institute for Molecules and Materials, Radboud University, 6525 ED Nijmegen, The Netherlands*

⁶*National Institute of Chemical Physics and Biophysics, Akadeemia tee 23, 12618 Tallinn, Estonia*

(Dated: June 11, 2018)

The optical magnetoelectric effect, which is an inherent attribute of the spin excitations in multiferroics, drastically changes their optical properties compared to conventional materials where light-matter interaction is expressed only by the dielectric permittivity and magnetic permeability. Our polarized absorption experiments performed on multiferroic $\text{Ca}_2\text{CoSi}_2\text{O}_7$ and $\text{Ba}_2\text{CoGe}_2\text{O}_7$ in the THz spectral range demonstrate that such magnetoelectric spin excitations show quadrochromism, i.e. they have different colours for all the four combinations of the two propagation directions (forward or backward) and the two orthogonal polarizations of a light beam. We found that quadrochromism can give rise to peculiar optical properties, such as one-way transparency and zero-reflection of these excitations, which can open a new horizon in photonics. One-way transparency is also related to the static magnetoelectric phenomena, hence, these optical studies can provide guidelines for the systematic synthesis of new materials with large dc magnetoelectric effect.

PACS numbers:

Nature offers a plethora of dichroic materials whose colour is different for two specific polarizations of the transmitted light. Dichroism generally appears in media which are not isotropic and provides information about their symmetry. Linear dichroism (absorption difference for two orthogonal linear polarizations of a light beam) emerges in materials where the symmetry is lower than cubic, while circular dichroism (absorption difference for the two circular polarizations) is observed in materials with finite magnetization or chiral structure. In all these cases the four transverse wave solutions obtained from the Maxwell equations for a given axis of light propagation group into two pairs, where each pair contains two counter-propagating waves ($\pm\mathbf{k}$) characterized by the same absorption coefficient.^{1,2}

In materials with simultaneously broken spatial inversion and time reversal symmetry this two-fold $\pm\mathbf{k}$ directional degeneracy of the Maxwell equations can be lifted and each of the four waves is absorbed with a different strength.³⁻⁷ Hereafter, we will refer to this phenomenon as quadrochromism and the corresponding materials as quadrochromic or four-coloured media. Following the early prediction of $\pm\mathbf{k}$ directional anisotropy^{4,8,9} and experimental observation^{10,11} of weak directional effects, recent optical studies on multiferroic materials report about strong directional dichroism in the GHz-THz^{6,12-15} and visible spectral range¹⁶⁻¹⁸ as a hallmark of quadrochromism.

I. RESULTS

Quadrochromism generated by the optical magnetoelectric effect. Here, we argue that the emergence

of quadrochromism is not a fortuitous issue but an inherent property of magnetoelectric multiferroics. In this class of materials, the coupling between the electric and magnetic states leads to the optical magnetoelectric effect described by the dynamical response functions $\hat{\chi}^{me}(\omega)$ and $\hat{\chi}^{em}(\omega)$.^{4-6,12,13,19} Consequently, an oscillating magnetization and polarization (M_i^ω and P_i^ω) are induced by the electric and magnetic components of light (E_i^ω and H_i^ω), respectively, besides the conventional terms arising from the dielectric permittivity ($\hat{\epsilon}$) and magnetic permeability ($\hat{\mu}$); $M_i^\omega = [\mu_{ij}(\omega) - 1]H_j^\omega + \sqrt{\epsilon_0/\mu_0}\chi_{ij}^{me}(\omega)E_j^\omega$ and $P_i^\omega = \epsilon_0[\epsilon_{ij}(\omega) - 1]E_j^\omega + \sqrt{\epsilon_0\mu_0}\chi_{ij}^{em}(\omega)H_j^\omega$. Solving the Maxwell equations with these generalized constitutive relations yields the following form of the complex refractive index for a given polarization (E_i^ω, H_j^ω):^{12,20}

$$N_{\pm}(\omega) \approx \sqrt{\epsilon_{ii}(\omega)\mu_{jj}(\omega)} \pm \frac{1}{2}[\chi_{ji}^{me}(\omega) + \chi_{ij}^{em}(\omega)], \quad (1)$$

where \pm signs correspond to wavevectors $\pm\mathbf{k}$. The second term in this formula explicitly shows the key role of the optical magnetoelectric effect in generating quadrochromism by lifting the $\pm\mathbf{k}$ degeneracy of the Maxwell equations. The derivation of Eq. 1 for magnetoelectric materials of various symmetries is given in the Methods section.

The optical magnetoelectric effect is exclusively generated by such transitions where both the electric- and magnetic-dipole moments induced by an absorbed pho-

ton are finite:

$$\chi_{ji}^{me}(\omega) = \frac{2}{V\hbar} \sqrt{\frac{\mu_0}{\epsilon_0}} \sum_n \left[\frac{\omega_{no} \Re\{\langle 0|m_j|n\rangle\langle n|p_i|0\rangle\}}{\omega_{no}^2 - \omega^2 - 2i\omega\delta} + \frac{i\omega \Im\{\langle 0|m_j|n\rangle\langle n|p_i|0\rangle\}}{\omega_{no}^2 - \omega^2 - 2i\omega\delta} \right] \triangleq \chi'_{ji}(\omega) + \chi''_{ji}(\omega), \quad (2)$$

i.e. the magnetic (m_j) and electric (p_i) dipole operators simultaneously must have non-vanishing matrix elements between the ground state $|0\rangle$ and the excited states $|n\rangle$ separated by $\hbar\omega_{no}$ energy. Here, V is the volume of the system, ϵ_0 and μ_0 are respectively the permittivity and the permeability of the vacuum. $\chi'_{ji}(\omega)$ and $\chi''_{ji}(\omega)$ are the sum of terms with the real (\Re) and the imaginary (\Im) parts of the matrix element products, respectively. The former changes sign under time reversal, while the latter remains invariant. Since the two cross effects are related by the Kubo formula according to $\chi_{ji}^{me}(\omega) = \chi'_{ji}(\omega) + \chi''_{ji}(\omega)$ and $\chi_{ij}^{em}(\omega) = \chi'_{ji}(\omega) - \chi''_{ji}(\omega)$, in Eq. 1 the time-odd $\chi'_{ji}(\omega)$ is solely responsible for the $\pm\mathbf{k}$ directional anisotropy; $N_+(\omega) - N_-(\omega) = \chi_{ji}^{me}(\omega) + \chi_{ij}^{em}(\omega) = 2\chi'_{ji}(\omega)$.

When the optical magnetoelectric effect is sufficiently strong, a four-coloured material can become fully transparent for a given propagation direction, while it still absorbs light beams traveling in the opposite direction. We define the magnetoelectric ratio for a given transition as $\gamma \triangleq \frac{\langle n|m_j|0\rangle}{\langle n|p_i|0\rangle}$. For a magnetoelectric resonance separated from other excitations the one-way transparency, that is $\alpha_-(\omega) \equiv \frac{2\omega}{c} \Im\{N_-(\omega)\} = 0$ while $\alpha_+(\omega) \equiv \frac{2\omega}{c} \Im\{N_+(\omega)\} \neq 0$ or vice versa, can occur for a given polarization E_i^ω if

$$\gamma = \pm \frac{c}{\sqrt{\epsilon_i^\infty}}, \quad (3)$$

where c is the speed of light in vacuum, ϵ_i^∞ is the dielectric permittivity due to optical transitions at higher frequencies. Note that one-way transparency is only possible when γ is purely real, i.e. the interference between the magnetic- and electric-dipole matrix elements has to be perfectly constructive or destructive. Correspondingly, the \pm signs refer to the two cases when the polarization and the magnetization induced by the electromagnetic field oscillate with zero and π phase difference, respectively. The condition in Eq. 3 can be equivalently expressed by the susceptibilities in the frequency region of the individual magnetoelectric transition, namely $\chi''_{ji}(\omega)$ has to vanish and the ratio of the dynamical magnetic and electric susceptibility needs to be equal to $1/\epsilon_i^\infty$. Note that in CGS units Eq. 3 has the form $\gamma = \pm \frac{1}{\sqrt{\epsilon_i^\infty}}$, hence, the magnetic- and electric-dipole matrix elements must be of the same order of magnitude to approach the one-way transparency. (For details see the Methods section.)

Although directional anisotropy is not manifested in the reflectivity of a vacuum-material interface at normal incidence, the one-way transparency of a bulk material

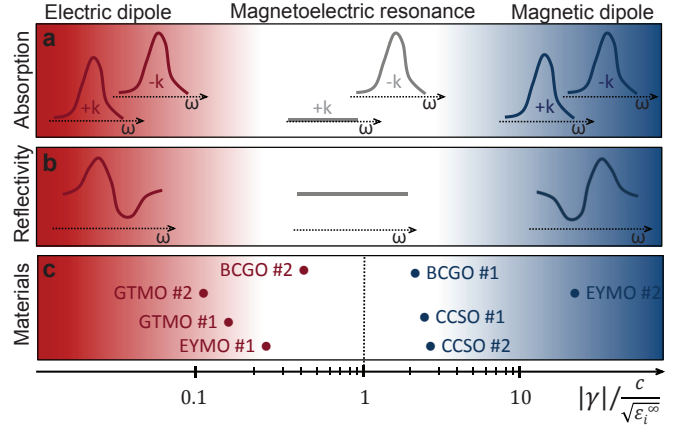


FIG. 1: | **One-way transparency at magnetoelectric resonances.** Optical properties characteristic to pure electric-dipole, mixed magnetoelectric and pure magnetic-dipole excitations corresponding to different values of the magnetoelectric ratio, γ . **a**, Counter-propagating beams are absorbed with the same strength in case of pure electric (red region) and magnetic (blue region) dipole transitions as illustrated by the two absorption peaks labeled with $+\mathbf{k}$ and $-\mathbf{k}$ (for clarity the two peaks are shifted relative to each other). When approaching the limit of ideal magnetoelectric resonance (white region), where $|\gamma| = c/\sqrt{\epsilon_i^\infty}$, the material tends to show one-way transparency. **b**, Electric- and magnetic-dipole transitions emerge with opposite line shapes in the reflectivity spectrum, while an ideal magnetoelectric resonance remains hidden. **c**, Magnetoelectric ratio for magnon modes with strong $\pm\mathbf{k}$ directional anisotropy observed in multiferroic $\text{Ca}_2\text{CoSi}_2\text{O}_7$ (CCSO), $\text{Ba}_2\text{CoGe}_2\text{O}_7$ (BCGO), $\text{Gd}_{0.5}\text{Tb}_{0.5}\text{MnO}_3$ (GTMO)¹⁵ and $\text{Eu}_{0.55}\text{Y}_{0.45}\text{MnO}_3$ (EYMO).¹⁴ For the mode assignments see the main text and Fig. 4. The γ values and their field dependence for the different modes are given in the Supplementary Fig. S1.

can still be accompanied by peculiar behaviour of the normal-incidence reflectivity, namely the magnetoelectric resonance remains hidden in the reflectivity spectrum, $R(\omega)$. Purely electric- and magnetic-dipole transitions appear in the reflectivity spectrum with opposite line shapes according to the Fresnel formula $R = \left| \frac{1 - \sqrt{\frac{\mu_{jj}}{\epsilon_{ii}}}}{1 + \sqrt{\frac{\mu_{jj}}{\epsilon_{ii}}}} \right|^2$ as schematically shown in Fig. 1. Thus, the relative strength of magnetic and electric susceptibilities for a given resonance can be determined from the shape of $R(\omega)$ near the resonance. When the condition $|\gamma| = c/\sqrt{\epsilon_i^\infty}$ is fulfilled the reflectivity spectrum is featureless at the resonance with the constant value of $R = \left| \frac{\sqrt{\epsilon_i^\infty} - 1}{\sqrt{\epsilon_i^\infty} + 1} \right|^2$ as if there was no resonance present in that frequency range. (See the Methods section.)

Multiferroic character of $\text{Ca}_2\text{CoSi}_2\text{O}_7$. This compound crystallizes in a non-centrosymmetric tetragonal $P\bar{4}2_1m$ structure^{21,22} where Co^{2+} cations with $S=3/2$ spin form square-lattice layers stacked along the tetragonal $[001]$ axis. The static magnetic and magnetoelec-

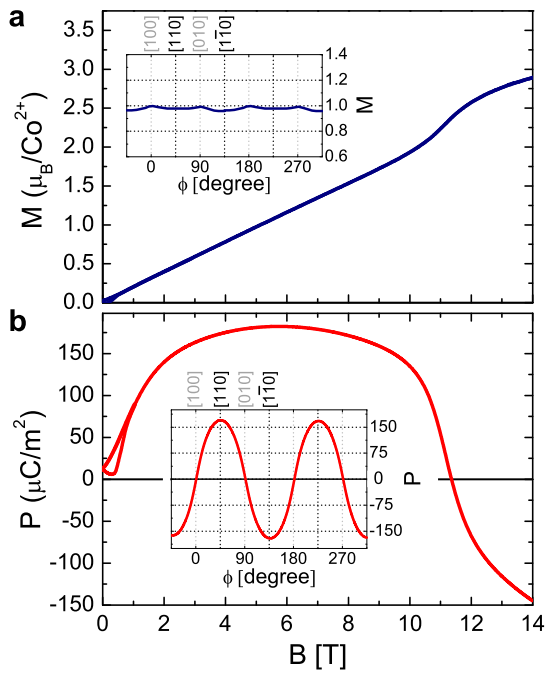


FIG. 2: | **Magnetoelectric properties of multiferroic $\text{Ca}_2\text{CoSi}_2\text{O}_7$ at $T=2\text{K}$.** Field dependence of **a**, the magnetization (M) and **b**, the ferroelectric polarization induced along the tetragonal $[001]$ axis (P) for magnetic fields parallel to the $[110]$ direction. There is a hysteresis in both quantities for fields $<1\text{T}$. The insets display the angular dependence of the magnetization and polarization when a magnetic field of $B=5\text{T}$ is rotated within the tetragonal plane.

tric properties of $\text{Ca}_2\text{CoSi}_2\text{O}_7$,^{23,24} as shown in Fig. 2, resemble to the properties of other multiferroic compounds from the same family such as $\text{Ba}_2\text{CoGe}_2\text{O}_7$ ^{25–29} and $\text{Sr}_2\text{CoSi}_2\text{O}_7$.³⁰ This material shows an antiferromagnetic ordering below $T_N=5.7\text{K}$ with a small ferromagnetic component of the spins (M) lying in the tetragonal plane.^{31,32} Below T_N , magnetic fields applied along the $[110]$ (or $[1\bar{1}0]$) axis of the tetragonal plane induce ferroelectric polarization along the $[001]$ direction (P), which changes sign at $B\approx 11\text{T}$ accompanied by an anomaly in the magnetization. The rotation of $B=5\text{T}$ magnetic field within the tetragonal plane results in a nearly sinusoidal modulation of P with zero crossing for fields pointing along the $[100]$ and $[010]$ axes. The variation of M is less than 5% implying that in-plane magnetic anisotropies, due to e.g. small orthorhombicity of the crystal structure, become negligible in this field range. On this basis we expect that the magnetic symmetry of the material can be approximated by the $mm'2'$ ($m'm'2'$) polar point group for $\mathbf{B}\parallel[110]$ ($\mathbf{B}\parallel[1\bar{1}0]$) and by the $2'2'2'$ ($2'2'2'$) chiral point group for $\mathbf{B}\parallel[100]$ ($\mathbf{B}\parallel[010]$) similarly to the multiferroic state of $\text{Ba}_2\text{CoGe}_2\text{O}_7$.^{12,13,29,33} (Prime denotes when a spatial symmetry is combined with the time reversal operation.) The role of toroidal order in the peculiar magnetoelectric phenomena emerging in the $mm'2'$ state of these compounds has also been

emphasized.³³

Four-coloured spin-wave excitations in $\text{Ca}_2\text{CoSi}_2\text{O}_7$ and $\text{Ba}_2\text{CoGe}_2\text{O}_7$. Using terahertz absorption spectroscopy we have investigated the $\pm\mathbf{k}$ directional anisotropy of spin-wave excitations (magnons) in the frequency range of $0.2 - 2\text{THz}$ ($0.8 - 8\text{meV}$) on single crystals of $\text{Ca}_2\text{CoSi}_2\text{O}_7$ and $\text{Ba}_2\text{CoGe}_2\text{O}_7$ up to as high magnetic fields as $B=30\text{T}$. Former studies on $\text{Ba}_2\text{CoGe}_2\text{O}_7$ have demonstrated the role of magnetoelectric phenomena in the THz optical properties of this material and reported about strong directional dichroism of the magnon excitations.^{12,13,19,34,35} To verify the quadrochroic nature of the magnons both the polarization and the $\pm\mathbf{k}$ directional dependence of the absorption have been studied. Since the $\chi'_{ji}(\omega)$ magnetoelectric tensor component responsible for the directional anisotropy is odd under time reversal, changing the sign of the static magnetic field applied in the experiments is equivalent to the reversal of light propagation direction. Therefore, we fixed the propagation direction and recorded the absorption spectra for $\pm\mathbf{B}$. All the absorption spectra have been measured in Faraday configuration, when the light propagates parallel or antiparallel to the external magnetic field.

While the static magnetic and magnetoelectric properties of $\text{Ca}_2\text{CoSi}_2\text{O}_7$ and $\text{Ba}_2\text{CoGe}_2\text{O}_7$ show close similarities, the nature of the spin-wave excitations is different in the two compounds as clearly followed in Fig. 3. In $\text{Ca}_2\text{CoSi}_2\text{O}_7$ the absorption of the magnon modes is weak in low fields and is gradually enhanced towards high fields accompanied by a strong blue shift. In contrast, the magnons in $\text{Ba}_2\text{CoGe}_2\text{O}_7$ show up with large intensity in low fields and the field dependence of the resonances is more complex. In both compounds some of the modes disappear in high magnetic fields.

Strong directional dichroism, i.e. different absorption for light beams propagating along and opposite to the magnetic field, has been observed in both cases. Moreover, the sign of the directional dichroism is reversed by changing the orientation of the sample from $\mathbf{B}\parallel[100]$ to $\mathbf{B}\parallel[010]$ by $\pi/2$ rotation of the crystal around the tetragonal axis (compare spectra in Fig. 3a and Fig. 3b). On the other hand, we have checked that rotating the crystal by π around any of the $[100]$, $[010]$ and $[001]$ axes during the measurement leaves the absorption spectra unchanged. These observations support our assignment that the symmetry of these materials corresponds to the $22'2'$ and $2'2'2'$ chiral point group for $\mathbf{B}\parallel[100]$ and $\mathbf{B}\parallel[010]$, respectively. Thus, the directional dichroism observed in Faraday configuration is the manifestation of the magnetically induced chiral state of matter. Magnetic switching between the same two chiral enantiomers ($22'2'$ and $2'2'2'$) in $\text{Ba}_2\text{CoGe}_2\text{O}_7$ has also been verified by the detection of strong natural circular dichroism for the magnon modes.¹³ Note that the spatial inversion and time reversal symmetry are simultaneously broken by the chirality and the magnetization of the material, respectively.

The four-coloured nature of the spin excitations in

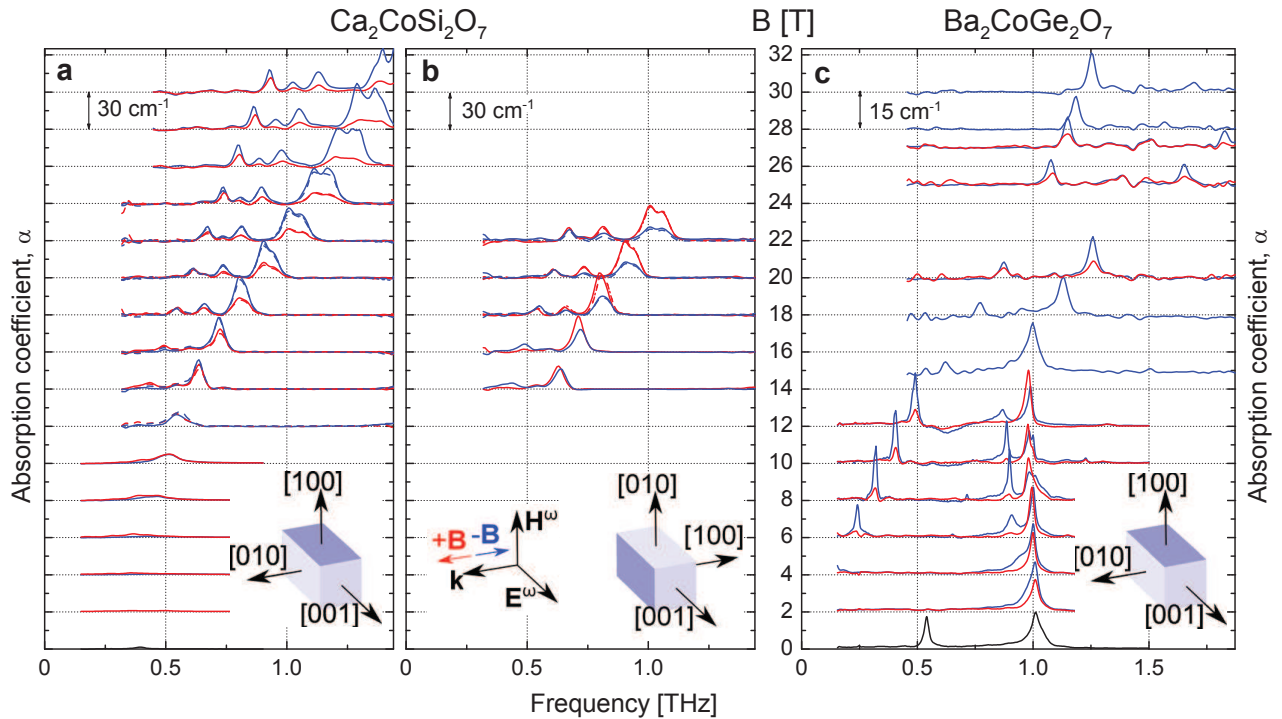


FIG. 3: | **Directional dichroism of the magnon modes in $\text{Ca}_2\text{CoSi}_2\text{O}_7$ and $\text{Ba}_2\text{CoGe}_2\text{O}_7$.** Absorption spectra measured in Faraday configuration, i.e. for $\mathbf{B} \parallel \mathbf{k}$, in magnetic fields $B=0\text{-}30$ T at $T=2$ K. The spectra are shifted vertically proportional to the magnitude of the field and the distance between horizontal grid lines is indicated in each panel. The axis of the static magnetic field together with the polarization and the propagation direction of light, common for all spectra in the figure, are shown in panel **b**, while the corresponding sample orientation is specified in each panel. In panel **a** and **c**, the polarization configuration is $\mathbf{E}^\omega \parallel [001]$, $\mathbf{H}^\omega \parallel [100]$ and $\mathbf{k} \parallel [010]$, while in panel **b**, the sample is rotated by $\pi/2$ around the $[001]$ axis. Red and blue spectra correspond to light propagation along and opposite to the magnetic field, respectively. In both materials, some of the modes exhibit strong directional ($\pm\mathbf{k}$) dichroism, absorption difference for counter-propagating light beams, almost realizing one-way transparency. Measurements on $\text{Ca}_2\text{CoSi}_2\text{O}_7$, shown in panel **a** and **b**, have been repeated after π rotations of the sample around the $[100]$, $[010]$ and $[001]$ axes. The corresponding spectra plotted with dashed lines nearly coincide with the original ones in the whole frequency range.

$\text{Ca}_2\text{CoSi}_2\text{O}_7$ and $\text{Ba}_2\text{CoGe}_2\text{O}_7$ is demonstrated in Fig. 4. The absorption spectra were measured in magnetic fields parallel and antiparallel to the propagation direction (being equivalent to the reversal of light propagation) for two orthogonal polarizations. For most of the magnon modes the strength of light absorption is different in all the four cases. When the crystals are rotated by $\pi/4$ around the $[001]$ axis, the materials are expected not to be chiral but polar, which was experimentally verified by the lack of $\pm\mathbf{k}$ directional anisotropy in Faraday configuration as shown in the Supplementary Fig. S2. In this case the spin excitations lose their quadrochroic character and become ordinary dichroic transitions.

One-way transparency of magnetoelectric transitions in multiferroics. As clear from Eq. 3, one-way transparency emerging in a finite spectral range is not a limit which would be protected by any fundamental law of nature. Indeed in multiferroics there are spin-wave excitations with magnetoelectric (both electric- and magnetic-dipole) character^{6,12–15,19,20} and even purely electric-dipole active spin excitations^{36–43} emerge besides the conventional magnon modes being only magnetic-

dipole active. While the ratio of the matrix elements can be mostly controlled via the spin system, ϵ_i^∞ is mainly determined by the lattice vibrations, i.e. the crystal structure of the material. Thus, one-way transparency can be achieved by tailored material synthesis.

The magnetoelectric ratio for a separate transition can be calculated from the absorption spectra measured for counter-propagating beams, $\alpha_+(\omega)$ and $\alpha_-(\omega)$, according to the following formula:

$$\gamma = \frac{c}{\sqrt{\epsilon_i^\infty}} \frac{\sqrt{\frac{\alpha_+}{\alpha_-}} \pm 1}{\sqrt{\frac{\alpha_+}{\alpha_-}} \mp 1}. \quad (4)$$

The upper/lower sign corresponds to the case when the transition is located at the magnetic/electric-dipole side of the border of one-way transparency, which can be determined from polarized reflectivity spectra as explained earlier or by the systematic polarization dependence of the absorption spectra. (See Methods section for the derivation of Eq. 4.)

Figure 1 shows the magnetoelectric ratio, γ for

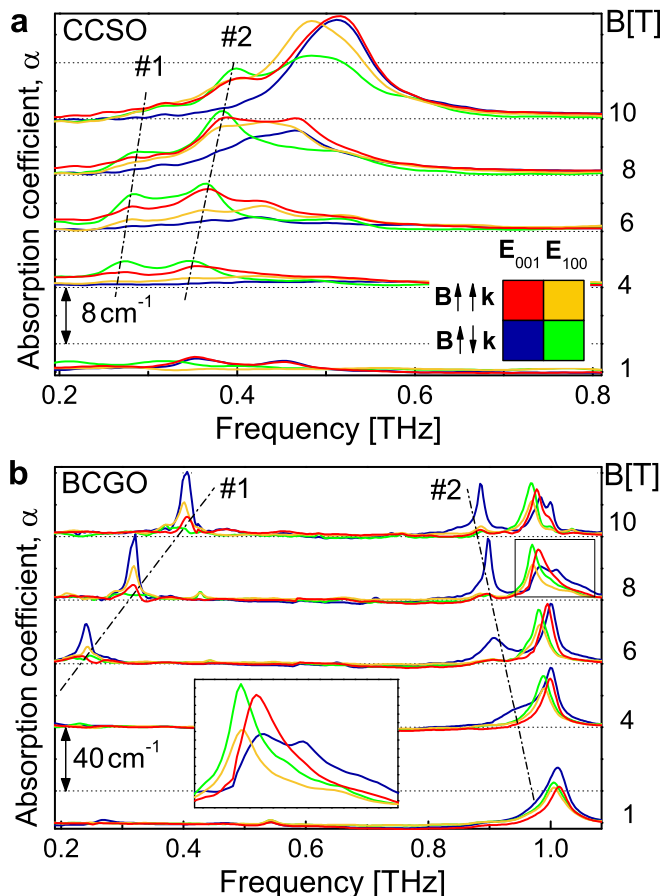


FIG. 4: | **Quadrochroic magnons in multiferroics.** THz absorption spectra of **a**, $\text{Ca}_2\text{CoSi}_2\text{O}_7$ (CCSO) and **b**, $\text{Ba}_2\text{CoGe}_2\text{O}_7$ (BCGO) measured in magnetic fields $\mathbf{B} \parallel \mathbf{k} \parallel [010]$ at $T=4\text{K}$. Spectra recorded in the four cases, i.e. for beams propagating along and opposite to the magnetic field direction in two orthogonal polarizations $\mathbf{E}^\omega \parallel [001]$ and $\mathbf{E}^\omega \parallel [100]$, are plotted with four different colours as explained in the inset of panel **a**. To clearly visualize that the absorption is different in all the four cases, the magnon modes in BCGO located in the 0.94-1.07 THz region are framed in the spectra measured in $B=8\text{T}$ and are enlarged in the inset of panel **b**. For both compounds, magnon modes with the strongest $\pm\mathbf{k}$ directional dichroism are indicated with dash-dotted lines and labeled as #1 and #2. Figure 1 and the main text refer to these modes in polarization $\mathbf{E}^\omega \parallel [001]$.

magnon modes with strong directional anisotropy in $\text{Ca}_2\text{CoSi}_2\text{O}_7$, $\text{Ba}_2\text{CoGe}_2\text{O}_7$ and for two other multiferroics $\text{Gd}_{0.5}\text{Tb}_{0.5}\text{MnO}_3$ and $\text{Eu}_{0.55}\text{Y}_{0.45}\text{MnO}_3$. The selected modes are separated from other transitions, hence, their magnetoelectric ratio can be determined according to Eqs. 3 & 4. For $\text{Ca}_2\text{CoSi}_2\text{O}_7$ and $\text{Ba}_2\text{CoGe}_2\text{O}_7$ the labeling of the modes follows the notation used in Fig. 4. GTMO #1 and EYMO #1 refer to the lowest-energy spin-current driven electromagnon in $\text{Gd}_{0.5}\text{Tb}_{0.5}\text{MnO}_3$ ¹⁵ and $\text{Eu}_{0.55}\text{Y}_{0.45}\text{MnO}_3$,¹⁴ respectively. GTMO #2 is the exchange-striction induced electromagnon^{36,38,40} and EYMO #2 is the con-

ventional antiferromagnetic resonance⁴⁴ both located at $\approx 0.6\text{-}0.7\text{THz}$. (The selection rules for these transitions are as specified in Refs. 14 & 15.). The magnetoelectric ratio could be unambiguously determined from the directional anisotropy data together with the systematic polarization dependence of the absorption spectra for the modes in $\text{Ba}_2\text{CoGe}_2\text{O}_7$ ^{12,13,34} and for the higher-energy modes in $\text{Gd}_{0.5}\text{Tb}_{0.5}\text{MnO}_3$ ^{15,38,40} and $\text{Eu}_{0.55}\text{Y}_{0.45}\text{MnO}_3$.^{14,44} The dominantly magnetic- and electric-dipole character of modes BCGO #1 and BCGO #2, respectively, is in agreement with the theoretical predictions.^{19,34} The spin excitations in $\text{Ca}_2\text{CoSi}_2\text{O}_7$ are tentatively assigned to the magnetic-dipole side of the $\gamma=c/\sqrt{\epsilon_i^\infty}$ boundary, while the spin-current driven mode in $\text{Gd}_{0.5}\text{Tb}_{0.5}\text{MnO}_3$ and $\text{Eu}_{0.55}\text{Y}_{0.45}\text{MnO}_3$ is assumed to be at the electric-dipole side. Note that the selected magnon modes in $\text{Ca}_2\text{CoSi}_2\text{O}_7$ and $\text{Ba}_2\text{CoGe}_2\text{O}_7$ show nearly one-way transparency as also evident from Fig. 4. Moreover, the high-field spectra in Fig. 3 show that the $\frac{\alpha_+}{\alpha_-}$ ratio is nearly the same for all the modes in $\text{Ca}_2\text{CoSi}_2\text{O}_7$, i.e. they are characterized by a uniform magnetoelectric ratio.

Connection between the directional dichroism spectrum and the dc magnetoelectric effect. The dc magnetoelectric susceptibility is a key parameter, which determines the feasibility of applying multiferroics in memories with fast low-power electrical write operation, and non-destructive non-volatile magnetic read operation.⁴⁵ Since the static and the dynamical responses of a system are intimately connected to each other, the study of the optical magnetoelectric effect can help the systematic synthesis of materials with large dc magnetoelectric effect. This connection is expressed by the Kramers-Kronig transformation of the dynamical magnetoelectric susceptibility when taking the zero-frequency limit:

$$\begin{aligned} \chi_{ij}^{me}(\omega=0) &= \frac{2}{\pi} \int_0^\infty \frac{\Im\{\chi_{ij}^{me}(\omega')\}}{\omega'} d\omega' \\ &= \frac{c}{2\pi} \int_0^\infty \frac{\alpha_+(\omega') - \alpha_-(\omega')}{\omega'^2} d\omega'. \end{aligned} \quad (5)$$

Hence, the static magnetoelectric coefficient is proportional to the integral of the directional dichroism over the whole frequency range. However, the ω'^2 denominator ensures that the main contribution comes from the lowest-frequency magnetoelectric excitations, i.e. from the magnon modes, if the contribution from domain dynamics is negligible. (The second equality in Eq. 5 holds only if $\chi_{ij}''(\omega) \equiv 0$, which is indeed the case for multiferroic compounds belonging to many magnetic point groups.)

II. DISCUSSION

We have demonstrated that quadrochroism generated by the optical magnetoelectric effect in multiferroics is an inherent property of the spin-wave excitations located

in the THz spectral range. By tuning the ratio of the magnetic and electric-dipole matrix elements the material can exhibit one-way transparency in the vicinity of the transition, while the resonance remains hidden in the reflectivity. The external control over the magnetization and the electric polarization in multiferroics facilitate the switching between the transparent and absorbing directions via static magnetic or electric fields. It has recently been predicted⁴⁶ and also observed⁴⁷ that the spin excitations of skyrmion crystals at microwave frequencies can also exhibit remarkable directional anisotropy.

Besides spin excitations, we expect that the optical magnetoelectric effect can strongly influence the optical properties of multiferroics in the infrared-visible region. Crystal field transitions of the d or f shell electrons of magnetic ions can show strong directional anisotropy as was observed in multiferroic CuB_2O_4 ^{16,17} and $(\text{Cu,Ni})\text{B}_2\text{O}_4$.¹⁸ While crystal-field excitations predominantly have an electric-dipole character, strong spin-orbit interaction can tune their magnetoelectric ratio close to $c/\sqrt{\epsilon_i^\infty}$.

In contrast to the common belief that lattice vibrations are purely electric-dipole active transitions, the optical magnetoelectric effect can also emerge for phonon modes in multiferroics as has recently been reported for the magnetoelectric atomic rotations in $\text{Ba}_3\text{NbFe}_3\text{Si}_2\text{O}_{14}$.⁴⁸ For completing the list of excitations, we recall that $\pm\mathbf{k}$ directional anisotropy was first observed for excitonic transitions of CdS by Hopfield and Thomas⁴⁹ in 1960. Since any of spin, orbital and lattice excitations can exhibit optical magnetoelectric effect in multiferroics, these new optical functionalities may work over a broad spectrum of the electromagnetic radiation from the THz range to the visible region.

III. METHODS

Polarized THz absorption spectroscopy. For the study of polarized absorption in magnetic fields up to 30 T we used Fourier transform spectroscopy. The measurement system for the B=0-12 T region is based on a Martin-Puplett interferometer, a mercury arc lamp as a light source, and a Si bolometer cooled down to 300 mK as a light intensity detector. This setup covers the spectral range 0.13-6 THz with a maximum resolution of 0.004 THz. The polarization of the beam incident to the sample is set by a wire-grid polarizer, while the detection side (light path from the sample till the detector) is insensitive to the polarization of light. Experiments up to 30 T were carried out at the THz facility of the High Field Magnet Laboratory in Nijmegen, where a Michelson interferometer is used together with a 1.6 K Si bolometer providing a spectral coverage of 0.3-6 THz.

All the measurements were carried out in Faraday configuration, i.e. by applying magnetic fields (anti)parallel to the direction of light propagation using oriented single crystal pieces with the typical thickness of 1 mm. The

crystals were grown by a floating-zone method and were characterized by magnetization and ferroelectric polarization experiments prior to the optical study.²⁵

Formulae for quadrochromism. The quadrochromism of spin excitations located in the long-wavelength region of light can be described by the Maxwell's equations

$$\begin{aligned}\omega\mathbf{B}^\omega &= \mathbf{k} \times \mathbf{E}^\omega, \\ -\omega\mathbf{D}^\omega &= \mathbf{k} \times \mathbf{H}^\omega,\end{aligned}$$

by introducing the dynamical magnetoelectric effects into the constitutive relations:

$$\begin{aligned}\mathbf{B}^\omega &= \hat{\mu}\mu_0\mathbf{H}^\omega + \hat{\chi}^{me}\sqrt{\epsilon_0\mu_0}\mathbf{E}^\omega, \\ \mathbf{D}^\omega &= \hat{\epsilon}\epsilon_0\mathbf{E}^\omega + \hat{\chi}^{em}\sqrt{\epsilon_0\mu_0}\mathbf{H}^\omega.\end{aligned}$$

The microscopic form of the dielectric permittivity ($\hat{\epsilon}$) and magnetic permeability ($\hat{\mu}$) is given by the Kubo formula:

$$\begin{aligned}\mu_{ji}(\omega) &= \delta_{ji} + \frac{2\mu_0}{V\hbar} \sum_n \left[\frac{\omega_{no}\Re\{\langle 0|m_j|n\rangle\langle n|m_i|0\rangle\}}{\omega_{no}^2 - \omega^2 - 2i\omega\delta} \right. \\ &\quad \left. + \frac{i\omega\Im\{\langle 0|m_j|n\rangle\langle n|m_i|0\rangle\}}{\omega_{no}^2 - \omega^2 - 2i\omega\delta} \right] \triangleq \mu'_{ji}(\omega) + \mu''_{ji}(\omega), \\ \epsilon_{ji}(\omega) &= \epsilon_i^\infty \delta_{ji} + \frac{2}{V\hbar\epsilon_0} \sum_n \left[\frac{\omega_{no}\Re\{\langle 0|p_j|n\rangle\langle n|p_i|0\rangle\}}{\omega_{no}^2 - \omega^2 - 2i\omega\delta} \right. \\ &\quad \left. + \frac{i\omega\Im\{\langle 0|p_j|n\rangle\langle n|p_i|0\rangle\}}{\omega_{no}^2 - \omega^2 - 2i\omega\delta} \right] \triangleq \epsilon'_{ji}(\omega) + \epsilon''_{ji}(\omega).\end{aligned}$$

Here, μ'_{ji} and ϵ'_{ji} are the sum of terms with the real (\Re) parts of the matrix element products (also including δ_{ji} and $\epsilon_i^\infty\delta_{ji}$, respectively) while, μ''_{ji} and ϵ''_{ji} are the sum of terms with the imaginary (\Im) parts of the matrix element products. In contrast to the parity of the magnetoelectric tensor introduced in Eq. 2, μ'_{ji} (ϵ'_{ji}) is invariant and μ''_{ji} (ϵ''_{ji}) changes sign under time reversal. ϵ_i^∞ is the background dielectric constant from modes located at higher frequencies than the studied frequency window, while magnetic permeability contribution from higher-frequency excitations is neglected being usually much smaller than unity.

Among crystals exhibiting $\pm\mathbf{k}$ directional anisotropy, the highest symmetry ones are chiral materials with the 432 cubic point group when magnetization develops along one of their principal axes. In this case their magnetic point symmetry is reduced to 42'2' where ' means the time-reversal operation. The four-fold rotational symmetry is preserved around the direction of the magnetization chosen as the y -axis in the following. According to Neumann's principle, for materials belonging to the $4_y2'_x2'_z$ point group the dynamical response tensors have the following form:

$$\begin{aligned}\hat{\mu} &= \begin{pmatrix} \mu'_{xx} & 0 & \mu'_{xz} \\ 0 & \mu'_{yy} & 0 \\ -\mu''_{xz} & 0 & \mu'_{xx} \end{pmatrix}, \quad \hat{\epsilon} = \begin{pmatrix} \epsilon'_{xx} & 0 & \epsilon'_{xz} \\ 0 & \epsilon'_{yy} & 0 \\ -\epsilon''_{xz} & 0 & \epsilon'_{xx} \end{pmatrix}, \\ \hat{\chi}^{me} &= \begin{pmatrix} \chi'_{xx} & 0 & \chi'_{xz} \\ 0 & \chi''_{yy} & 0 \\ -\chi'_{xz} & 0 & \chi''_{xx} \end{pmatrix},\end{aligned}$$

and the general relation $\chi_{ji}^{em}(\omega) = \chi'_{ij}(\omega) - \chi''_{ij}(\omega)$ yields in the present symmetry $\hat{\chi}^{em}(\omega) = -\hat{\chi}^{me}(\omega)$. By solving the Maxwell equations for propagation parallel and antiparallel to the magnetization direction ($\pm \mathbf{k} \parallel \mathbf{y}$), one obtains the following refractive indices for the left (\mathbf{E}_l^ω) and right (\mathbf{E}_r^ω) circularly polarized eigenmodes:

$$\begin{aligned} N_\pm^l &= \sqrt{(\epsilon'_{xx} \pm i\epsilon''_{xz})(\mu'_{xx} \pm i\mu''_{xz})} + i\chi''_{xx} \mp \chi'_{xz}, \\ N_\pm^r &= \sqrt{(\epsilon'_{xx} \mp i\epsilon''_{xz})(\mu'_{xx} \mp i\mu''_{xz})} - i\chi''_{xx} \mp \chi'_{xz}. \end{aligned}$$

The reflectivity of an interface between the vacuum and a material with $42'2'$ symmetry can be determined from the Maxwell equations in the usual way by using the boundary conditions. For normal incidence the components of the magnetoelectric tensor do not appear in the reflectivity and one can reproduce the general expression:

$$R^{l/r} = \left| \frac{1 - Z^{l/r}}{1 + Z^{l/r}} \right|^2,$$

where $Z^{l/r} = Z_0 \sqrt{\frac{\mu_{xx} \pm i\mu_{xy}}{\epsilon_{xx} \pm i\epsilon_{xy}}}$ and Z_0 are the surface impedance of the interface and the impedance of vacuum, respectively. Keeping only the leading term in the surface impedance, i.e. $Z = Z_0 \sqrt{\mu_{jj}/\epsilon_{ii}}$ for polarization E_i^ω , the expression for the normal-incidence reflectivity given above is generally valid for materials belonging to other magnetic point groups as well.

When the symmetry is reduced to $2_y 2'_x 2'_z$, as is the case in the magnetically induced chiral state of $\text{Ca}_2\text{CoSi}_2\text{O}_7$ and $\text{Ba}_2\text{CoGe}_2\text{O}_7$, the equivalence of x - and z -axis does not hold anymore. Consequently the form of the tensors changes and the eigenmodes become elliptically polarized. Since the (100) plane studied for these materials shows strong linear dichroism/birefringence due to their crystal structure (with a dielectric constant $\epsilon^\infty \approx 12$ and 8 for polarizations along the optical axes [100] and [001], respectively, as determined from transmission data), the eigenmodes are expected to be nearly linearly polarized. The approximate form of the refractive index, when keeping only the time-reversal odd components of $\hat{\chi}^{me}$ and the time-reversal even components in $\hat{\epsilon}$ and $\hat{\mu}$ (i.e. neglecting polarization rotation):

$$\begin{aligned} N_\pm^1 &\approx \sqrt{\epsilon'_{zz}\mu'_{xx}} \pm \chi'_{xz}, \\ N_\pm^2 &\approx \sqrt{\epsilon'_{xx}\mu'_{zz}} \mp \chi'_{zx}. \end{aligned}$$

In a broad class of orthorhombic multiferroics the magnetization and ferroelectric polarization are perpendicular to each other. Choosing the magnetization and polarization parallel to the y -axis and z -axis, respectively, the magnetic point group is the $m_{xz}m'_{yz}2'_z$. In this case, the form of $\hat{\epsilon}$ and $\hat{\mu}$ tensors is the same as in $4_y 2'_x 2'_z$ but the magnetoelectric tensors become different:

$$\hat{\chi}^{me} = \begin{pmatrix} 0 & \chi''_{xy} & 0 \\ \chi''_{yx} & 0 & \chi'_{yz} \\ 0 & \chi'_{zy} & 0 \end{pmatrix}.$$

For propagation perpendicular both to the direction of the magnetization and the ferroelectric polarization ($\pm \mathbf{k} \parallel \mathbf{x}$), the refractive indices for the two linearly polarized eigenmodes (\mathbf{E}_z^ω and \mathbf{E}_y^ω):

$$\begin{aligned} N_\pm^z &= \sqrt{\frac{\epsilon'_{xx}\epsilon'_{zz} + \epsilon''_{xz}{}^2}{\epsilon'_{xx}}} \left[\frac{(\chi''_{yx})^2}{\epsilon'_{xx}} + \mu'_{yy} \right] \pm \left(\chi'_{yz} - \chi''_{yx} \frac{\epsilon''_{xz}}{\epsilon'_{xx}} \right) \\ &\approx \sqrt{\epsilon'_{zz}\mu'_{yy}} \pm \chi'_{yz}, \\ N_\pm^y &= \sqrt{\frac{\mu'_{xx}\mu'_{zz} + \mu''_{xz}{}^2}{\mu'_{xx}}} \left[\frac{(\chi''_{xy})^2}{\mu'_{xx}} + \epsilon'_{yy} \right] \mp \left(\chi'_{zy} - \chi''_{xy} \frac{\mu''_{xz}}{\mu'_{xx}} \right) \\ &\approx \sqrt{\epsilon'_{yy}\mu'_{zz}} \mp \chi'_{zy}. \end{aligned}$$

While in the lowest-order approximation the general formulae are $N_\pm^1 \approx \sqrt{\epsilon'_{ii}\mu'_{jj}} \pm \chi'_{ji}$ and $N_\pm^2 \approx \sqrt{\epsilon'_{jj}\mu'_{ii}} \mp \chi'_{ij}$ as given in Eq. 1, quadrichroism can be generated by other higher-order terms, such as $\chi''_{yx} \frac{\epsilon''_{xz}}{\epsilon'_{xx}}$, odd both in time reversal and spatial inversion. Note that ' and '' corresponds to the part of $\hat{\chi}^{me}$ being odd and even under time reversal, respectively, while the situation is reversed for $\hat{\mu}$ and $\hat{\epsilon}$.

Criterion of one-way transparency. We calculate the absorption coefficient in the vicinity of a separate magnetoelectric resonance, i.e. when the photon with the frequency $\omega = \omega_{n0}$ resonantly excites the $|0\rangle \rightarrow |n\rangle$ transition. When using the Kubo formula for $\hat{\chi}^{me}$, $\hat{\mu}$ and $\hat{\epsilon}$, the refractive index for a given polarization, $N_\pm \approx \sqrt{\epsilon'_{ii}\mu'_{jj}} \pm \chi'_{ji}$, has the following form:

$$\begin{aligned} N_\pm &= \sqrt{\left(\epsilon_i^\infty + \frac{i}{V\hbar\epsilon_0\Gamma} |\langle n|p_i|0\rangle|^2 \right) \left(1 + \frac{i\mu_0}{V\hbar\Gamma} |\langle n|m_j|0\rangle|^2 \right)} \\ &\pm \frac{i}{V\hbar\Gamma} \sqrt{\frac{\mu_0}{\epsilon_0}} \langle 0|m_j|n\rangle \langle n|p_i|0\rangle \\ &\approx \sqrt{\epsilon_i^\infty} + \frac{i}{2V\hbar\Gamma} \sqrt{\frac{\mu_0}{\epsilon_0}} \left(\frac{c}{\sqrt{\epsilon_i^\infty}} + \frac{\sqrt{\epsilon_i^\infty}}{c} |\gamma|^2 \pm 2\xi |\gamma| \right) \\ &\times |\langle n|p_i|0\rangle|^2, \end{aligned} \quad (6)$$

where Γ is the line width of the transition and the square root in the first term is expanded up to second order. Then, the absorption coefficient vanishes for one direction, i.e. $\alpha_-(\omega) = \frac{2\omega}{c} \Im\{N_-(\omega)\} = 0$ or $\alpha_+(\omega) = \frac{2\omega}{c} \Im\{N_+(\omega)\} = 0$, if

$$|\gamma| = \frac{c}{\sqrt{\epsilon_i^\infty}} (\xi \pm \sqrt{\xi^2 - 1}), \quad (7)$$

where c is the speed of light in vacuum, ϵ_i^∞ is the dielectric permittivity for the given polarization due to other optical transitions and $\xi = \Re\{\gamma\}/|\gamma|$. Note that one-way transparency is only possible when γ is purely real corresponding to $\xi = +1$ or -1 and the formula simplifies to $|\gamma| = c/\sqrt{\epsilon_i^\infty}$ as given in Eq. 3. Note that γ is real when $\chi''_{ij} = 0$, which is the case for many multiferroic materials

belonging to different magnetic point groups. When γ is real Eq. 4 can be straightforwardly derived from Eq. 6. When the condition of one-way transparency holds for a separate resonance in a given polarization E_i^ω , the surface impedance does not change near the resonance and

has the frequency independent $Z=1/\sqrt{\epsilon_i^\infty}$ value. Thus, the reflectivity also coincides with the background value

$$R = \left| \frac{\sqrt{\epsilon_i^\infty - 1}}{\sqrt{\epsilon_i^\infty + 1}} \right|^2.$$

-
- ¹ Barron, L.D. *Molecular Light Scattering and Optical Activity*, (Cambridge University Press, Cambridge, 2004).
- ² Azzam, R.M.A. & Bashara, N.M. *Ellipsometry and polarized light* (North-Holland, Amsterdam) 1979.
- ³ Hornreich, R.M. & Shtrikman, S. Theory of gyrotropic birefringence. *Phys. Rev.* **171**, 1065-1074 (1968).
- ⁴ O'Dell, T.H. *The Electrodynamics of Magnetolectric Media* (North-Holland, Amsterdam), 1970.
- ⁵ Arima, T. Magneto-electric optics in non-centrosymmetric ferromagnets. *J. Phys.: Condens. Matter.* **20**, 434211 (2008).
- ⁶ Cano, A. Theory of electromagnon resonances in the optical response of spiral magnets. *Phys. Rev. B* **80**, 180416(R) (2009).
- ⁷ Szaller, D., Bordacs, S. & Kezsmarki, I. Symmetry conditions for nonreciprocal light propagation in magnetic crystals. *Phys. Rev. B* **87**, 014421 (2013).
- ⁸ Baranova, N.B. & Zeldovich, B.Ya. Theory of a new linear magnetorefractive effect in liquids. *Molec. Phys.* **38**, 1085-1098 (1979).
- ⁹ Barron, L.D. & Vrbancich, Magneto-chiral birefringence and dichroism. *Molec. Phys.* **51**, 715-730 (1984).
- ¹⁰ Rikken G.L.J.A. & Raupach, E. Observation of magneto-chiral dichroism. *Nature* **390**, 493-494 (1997).
- ¹¹ Rikken, G.L.J.A., Strohm, C. & Wyder, P. Observation of Magnetolectric Directional Anisotropy. *Phys. Rev. Lett.* **89**, 133005 (2002).
- ¹² Kezsmarki, I. et al. Enhanced Directional Dichroism of Terahertz Light in Resonance with Magnetic Excitations of the Multiferroic Ba₂CoGe₂O₇ Oxide Compound. *Phys. Rev. Lett.* **106**, 057403 (2011).
- ¹³ Bordacs, S. et al. Chirality of matter shows up via spin excitations. *Nat. Phys.* **8**, 734 (2012).
- ¹⁴ Takahashi, Y., Shimano, R., Kaneko, Y., Murakawa, H. & Tokura, Y. Magnetolectric resonance with electromagnons in a perovskite helimagnet. *Nat. Phys.* **8**, 121 (2012).
- ¹⁵ Takahashi, Y., Yamasaki Y. & Tokura, Y. Terahertz Magnetolectric Resonance Enhanced by Mutual Coupling of Electromagnons. *Phys. Rev. Lett.* **111**, 037204(2013).
- ¹⁶ Saito, M., Ishikawa, K., Taniguchi, K. & Arima, T. Magnetic Control of Crystal Chirality and the Existence of a Large Magneto-Optical Dichroism Effect in CuB₂O₄. *Phys. Rev. Lett.* **101**, 117402 (2008).
- ¹⁷ Saito, M., Taniguchi, K. & Arima, T. Gigantic Optical Magnetolectric Effect in CuB₂O₄. *J. Phys. Soc. Jpn.* **77**, 013705 (2008).
- ¹⁸ M. Saito, K. Ishikawa, S. Konno, K. Taniguchi & T. Arima, Periodic rotation of magnetization in a non-centrosymmetric soft magnet induced by an electric field. *Nat. Mater.* **8**, 634 (2009).
- ¹⁹ Miyahara, S. & Furukawa, N. Theory of magnetolectric resonance in two-dimensional S = 3/2 antiferromagnet Ba₂CoGe₂O₇ via spin-dependent metal-ligand hybridization mechanism. *J. Phys. Soc. Jpn.* **80**, 073708 (2011).
- ²⁰ Miyahara, S. & Furukawa, N. Nonreciprocal Directional Dichroism and Toroidal magnons in Helical Magnets. *J. Phys. Soc. Jpn.* **81**, 023712 (2012).
- ²¹ Hagiya, K., Ohmasa, M. & Iishi, K. The Modulated Structure of Synthetic Co-Akermanite, Ca₂CoSi₂O₇. *Acta Cryst.* **B49**, 172-179 (1993).
- ²² Jia, Z.H., Schaper, A.K., Massa, W., Treutmann, W. & Ragera H. Structure and phase transitions in Ca₂CoSi₂O₇-Ca₂ZnSi₂O₇ solid-solution crystals. *Acta Cryst.* **B62**, 547555 (2006).
- ²³ Akaki, M., Tozawa, J., Akahoshi, D. & Kuwahara, H. Gigantic magnetolectric effect caused by magnetic-field-induced canted antiferromagnetic-paramagnetic transition in quasi-two-dimensional Ca₂CoSi₂O₇ crystal. *Appl. Phys. Lett.* **94**, 212904 (2009).
- ²⁴ Akaki, M., Tozawa, J., Akahoshi, D. & Kuwahara, H. Magnetic and dielectric properties of A₂CoSi₂O₇ (A=Ca, Sr, Ba) crystals. *J. Phys. C* **150**, 042001 (2009).
- ²⁵ Murakawa, H., Onose, Y., Miyahara, S., Furukawa, N. & Tokura, Y. Ferroelectricity Induced by Spin-Dependent Metal-Ligand Hybridization in Ba₂CoGe₂O₇. *Phys. Rev. Lett.* **103**, 137202 (2010).
- ²⁶ Yi, H.T., Choi, Y.J., Lee, S. & Cheong, S.W. Multiferroicity in the square-lattice antiferromagnet of Ba₂CoGe₂O₇. *Appl. Phys. Lett.* **92**, 212904 (2008).
- ²⁷ Romhanyi, J., Lajko, M. & Penc, K. Zero- and finite-temperature mean field study of magnetic field induced electric polarization in Ba₂CoGe₂O₇: Effect of the antiferroelectric coupling. *Phys. Rev. B* **84**, 224419 (2011).
- ²⁸ Yamauchi, K., Barone, P. & Silvia Picozzi, S. Theoretical investigation of magnetolectric effects in Ba₂CoGe₂O₇. *Phys. Rev. B* **84**, 165137 (2011).
- ²⁹ Perez-Mato, J.M. & Ribeiro, J.L. On the symmetry and the signature of atomic mechanisms in multiferroics: the example of Ba₂CoGe₂O₇. *Acta Cryst.* **A67**, 264268 (2011).
- ³⁰ Akaki, M., Iwamoto, H., Kihara, T., Tokunaga, M. & Kuwahara H. Multiferroic properties of an akermanite Sr₂CoSi₂O₇ single crystal in high magnetic fields. *Phys. Rev. B* **86**, 060413(R) (2012).
- ³¹ Zheludev, A. et al. Spin Waves and the Origin of Commensurate Magnetism in Ba₂CoGe₂O₇. *Phys. Rev. B* **68**, 024428 (2003).
- ³² Hutanu, V. et al. Determination of the magnetic order and the crystal symmetry in the multiferroic ground state of Ba₂CoGe₂O₇. *Phys. Rev. B* **86**, 104401 (2012).
- ³³ Toledano, P., Khalyavin, D.D. & Chapon, L.C. Spontaneous toroidal moment and field-induced magnetotoroidic effects in Ba₂CoGe₂O₇. *Phys. Rev. B* **84**, 094421 (2011).
- ³⁴ Penc, K. et al. Spin-Stretching Modes in Anisotropic Magnets: Spin-Wave Excitations in the Multiferroic Ba₂CoGe₂O₇. *Phys. Rev. Lett.* **108**, 257203 (2012).
- ³⁵ Romhanyi, J. & Penc, K. Multiboson spin-wave theory for Ba₂CoGe₂O₇: A spin-3/2 easy-plane Neel antiferromagnet with strong single-ion anisotropy. *Phys. Rev. B* **86**, 174428 (2012).

- ³⁶ Pimenov, A. *et al.* Possible evidence for electromagnons in multiferroic manganites. *Nat. Phys.* **2**, 97-100 (2006).
- ³⁷ Sushkov, A.B., Mostovoy, M., Valdes Aguilar, R., Cheong, S.-W. & Drew, D. Electromagnons in multiferroic RMn_2O_5 compounds and their microscopic origin. *J. Phys.: Condens. Matter.* **20**, 434210 (2008).
- ³⁸ Takahashi, Y. *et al.* Evidence for an Electric-Dipole Active Continuum Band of Spin Excitations in Multiferroic TbMnO_3 . *Phys. Rev. Lett.* **101**, 187201 (2008).
- ³⁹ Valdes Aguilar, R. *et al.* Origin of Electromagnon Excitations in Multiferroic RMnO_3 . *Phys. Rev. Lett.* **102**, 047203 (2009).
- ⁴⁰ Kida, N. *et al.* Terahertz time-domain spectroscopy of electromagnons in multiferroic perovskite manganites. *J. Opt. Soc. Am. B* **26**, A35-A51 (2009).
- ⁴¹ Mochizuki, M., Furukawa, N. & Nagaosa, N. Theory of Electromagnons in the Multiferroic Mn Perovskites: The Vital Role of Higher Harmonic Components of the Spiral Spin Order. *Phys. Rev. Lett.* **104**, 177206 (2010).
- ⁴² Seki, S., Kida, N., Kumakura, S., Shimano, R. & Tokura, Y. Electromagnons in the Spin Collinear State of a Triangular Lattice Antiferromagnet. *Phys. Rev. Lett.* **105**, 097207 (2010).
- ⁴³ Kida, N., Kumakura, S., Ishiwata, S., Taguchi, Y. & Tokura, Y. Gigantic terahertz magnetochromism via electromagnons in the hexaferrite magnet $\text{Ba}_2\text{Mg}_2\text{Fe}_{12}\text{O}_{22}$. *Phys. Rev. B* **83**, 064422 (2011).
- ⁴⁴ Takahashi, Y. *et al.* Far-infrared optical study of electromagnons and their coupling to optical phonons in $\text{Eu}_{1-x}\text{Y}_x\text{MnO}_3$ ($x=0.1, 0.2, 0.3, 0.4, \text{ and } 0.45$). *Phys. Rev. B* **79**, 214431 (2009).
- ⁴⁵ Martin, L.W. *et al.* Advances in the growth and characterization of magnetic, ferroelectric, and multiferroic oxide thin films. *Mater. Sci. Eng. R* **68**, 89 (2010).
- ⁴⁶ Mochizuki, M. & Seki S. Magnetoelectric resonances and predicted microwave diode effect of the skyrmion crystal in a multiferroic chiral-lattice magnet. *Phys. Rev. B* **87**, 134403 (2013).
- ⁴⁷ Y. Okamura *et al.* Microwave magnetoelectric effect via skyrmion resonance modes in a helimagnetic multiferroic. *Nat. Commun.* **4**, 2391 (2013).
- ⁴⁸ Chaix, L. *et al.* THz Magnetoelectric Atomic Rotations in the Chiral Compound $\text{Ba}_3\text{NbFe}_3\text{Si}_2\text{O}_{14}$. *Phys. Rev. Lett.* **110**, 157208 (2013).
- ⁴⁹ Hopfield, J.J. & Thomas, D.G. Photon Momentum Effects in the Magneto-Optics of Excitons. *Phys. Rev. Lett.* **4**, 357-359 (1960).

Acknowledgements

We thank K. Penc and S. Miyahara for discussions. This work was supported by Hungarian Research Funds OTKA K108918, by KAKENHI, MEXT of Japan, by Funding Program for World-Leading Innovation R&D on Science and Technology (FIRST program) on "Quantum Science on Strong Correlation", by the Estonian Ministry of Education and Research under Grant SF0690029s09, and Estonian Science Foundation under Grants ETF8170 and ETF8703, by the bilateral program of the Estonian and Hungarian Academies of Sciences, by EuroMagNET II under the EU Contract No. 228043 and by HFML-RU/FOM, member of the European Magnetic Field Laboratory.

Author contributions

D.Sz., S.B., I.K., T.R., U.N., H.E. performed the THz experiments. H.M. synthesized the samples and carried out dc magnetoelectric measurements. All the authors contributed to the analysis and discussions of the results. I.K. wrote the manuscript and supervised the project.

Additional information

The authors declare no competing financial interests.